Free-Breathing Radial 3D Fat-Suppressed T1-Weighted Gradient Echo Sequence

A Viable Alternative for Contrast-Enhanced Liver Imaging in Patients Unable to Suspend Respiration

Hersh Chandarana, MD, Tobias K. Block, PhD,† Andrew B. Rosenkrantz, MD,* Ruth P. Lim, MBBS, MMed, FRANZCR,* Danny Kim, MD,* David J. Mossa, BS,* James S. Babb, PhD,* Berthold Kiefer, PhD,† and Vivian S. Lee, MD, PhD**

Objective: To compare free-breathing radially sampled 3D fat suppressed T1-weighted gradient-echo acquisitions (radial volumetric interpolated breath-hold examination [VIBE]) with breath-hold (BH) and free-breathing conventional (rectilinearly sampled k-space) VIBE acquisitions for postcontrast imaging of the liver.

Materials and Methods: Eighteen consecutive patients referred for clinically indicated liver magnetic resonance imaging were imaged at 3 T. Three minutes after a single dose of gadolinium contrast injection, free-breathing radial VIBE, BH VIBE, and free-breathing VIBE with 4 averages were acquired in random order with matching sequence parameters. Radial VIBE was acquired with the "stack-of-stars" scheme, which uses conventional sampling in the slice direction and radial sampling in-plane.

All image data sets were evaluated independently by 3 radiologists blinded to patient and sequence information. Each reader scored the following parameters: overall image quality, respiratory motion artifact, pulsation artifact, liver edge sharpness, and hepatic vessel clarity using a 5-point scale, with the highest score indicating the most optimum examination. Mixed model analysis of variance was used to compare sequences in terms of each measure of image quality.

Results: When scores were averaged over readers, there was no statistically significant difference between radial VIBE and BH VIBE regarding overall image quality ($P = 0.1015$), respiratory motion artifact ($P = 1.0$), and liver edge sharpness ($P = 0.2955$). Radial VIBE demonstrated significantly lower pulsation artifact ($P < 0.0001$), but had lower hepatic vessel clarity ($P = 0.0176$), when compared with BH VIBE. Radial VIBE had significantly higher image quality scores for all parameters when compared with free-breathing VIBE ($P < 0.0001$). Acquisition time for BH VIBE was 14 seconds and that of free-breathing radial VIBE and conventional VIBE with multiple averages was 56 seconds each.

Conclusion: Radial VIBE can be performed during free breathing for contrast-enhanced imaging of the liver with comparable image quality to BH VIBE. However, further work is necessary to shorten the acquisition time to perform dynamic imaging.

Key Words: liver MRI, free-breathing radial T1-weighted gradient echo sequence, radial volumetric interpolated breath-hold (radial VIBE) sequence

(*Invest Radiol* 2011;46: 648–653)

Received January 27, 2011, and accepted for publication, after revision, April 9, 2011.

From the *New York University Langone Medical Center, Departments of Radiology, 550 First Avenue, New York, NY; and †MR Application and Workflow Development, Siemens AG Healthcare Sector, Erlangen, Germany.

Conflicts of interest and sources of funding: none declared.

Reprints: Hersh Chandarana, MD, New York University Langone Medical Center, Department of Radiology, 550 First Ave, HW201, New York, NY 10016. E-mail: hersh.chandarana@nyumc.org.

ISSN: 0020-9996/11/4610-0648

Physiologic and bulk motion, including respiratory motion, cardiac pulsation, and bowel peristalsis, can degrade the image quality of an upper abdominal MRI examination and can render images nondiagnostic.[1–5] Motion artifacts can blur anatomic details such as liver edge and intrahepatic vessels.[6] Significant progress has been made over the last decade in overcoming motion-related artifacts, and various strategies have been proposed including imaging during suspended respiration,[7–9] acquiring images with navigator-gated schemes,[10–17] respiratory-ordered phase encoding,[18] gradient moment nulling,[19] and periodically rotated overlapping parallel lines with enhanced reconstruction (PROPELLER) technique.[20,21] The PROPELLER technique acquires k-space data in blades using a radial-type readout scheme that is less sensitive to motion. It has demonstrated substantial reduction in respiratory motion-related artifacts and improved image quality for 2-dimensional (2D) T2-weighted turbo spin-echo as well as diffusion-weighted imaging of the liver.[20,22,23]

To our knowledge, a radial approach has not been systematically investigated in clinical practice for 3-dimensional fat-suppressed T1-weighted interpolated spoiled gradient-echo (VIBE, volumetric interpolated BH examination) acquisition, which is the conventional sequence used for contrast-enhanced MR (magnetic resonance) examinations of the liver. Contrast-enhanced VIBE imaging is essential for liver lesion detection and characterization[24,25] and is routinely acquired as a BH acquisition. In patients with diminished BH capacity, such as elderly, debilitated, or pediatric patients, this approach results in substantially compromised image quality. A respiratory-navigated free-breathing 3D T1-weighted technique has been proposed as an alternative to BH examination.[26,27] However, respiratory-navigated sequences can result in unpredictably long acquisition times in patients with erratic breathing patterns and hence may not be ideal for contrast-enhanced imaging of the liver and upper abdomen where acquiring images at a particular time after contrast administration may be of essence.

Recently, a modified version of the VIBE sequence has been developed that uses the "stack-of-stars" scheme[28,29] to acquire the k-space data. It performs conventional sampling in the slice direction but uses radial readouts for each partition; such that the data is acquired along overlapping spokes or radial views (Fig. 1).

The purpose of our study was to assess the image quality of free-breathing radial VIBE for liver imaging after gadolinium injection and to compare with an alternative free-breathing algorithm, (rectilinear sampled) VIBE with multiple averages. We compared both free-breathing methods to conventional (rectilinear sampled) BH VIBE in patients with normal breath-holding capacity undergoing clinically indicated contrast-enhanced liver MRI.

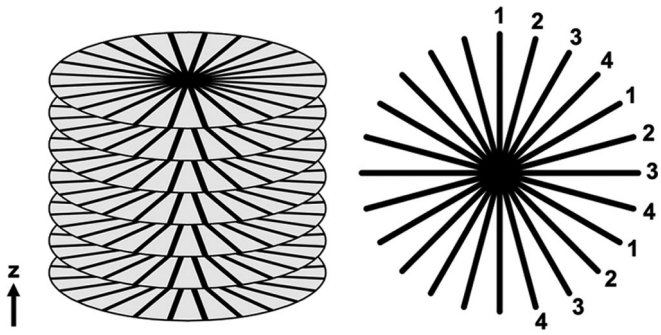

FIGURE 1. The stack-of-stars trajectory of the radial VIBE sequence (left) uses rectilinear sampling in the z-direction and radial sampling in the xy-plane. For each xy-plane, radial views are acquired in interleaves (right) where the numbers indicate the temporal ordering of the spokes.

MATERIALS AND METHODS

Patient Population

This Health Insurance Portability and Accountability Act (HIPAA)-compliant prospective single center study was performed after obtaining approval from our institutional review board. All patients provided written informed consent. Between September 2010 and December 2010, patients who presented to our department for clinically indicated liver MRI and who were scanned on a single 3 T MRI system (Magnetom Verio, Siemens Healthcare, Erlangen, Germany) on which the radial-VIBE sequence is available were enrolled.

Eighteen consecutive patients (11 M, 7 F; mean age, 52 years; range, 30–71 years) constituted our study cohort and were imaged for a variety of clinical indications: viral hepatitis and/or cirrhosis (n = 7), focal liver lesion (n = 4), abnormal liver function tests (n = 3), follow-up after liver transplant (n = 2), and abdominal pain (n = 2). None of the patients were known to have diminished breath-holding capacity.

MR Imaging

MR imaging was performed in all patients on a 3 T clinical system using torso phased array coils. All subjects underwent a routine liver imaging protocol that included conventional fast T1- and T2-weighted imaging and diffusion-weighted imaging. All patients then underwent axial 3D T1-weighted gradient echo fat suppressed acquisition before and after injection of gadopentetate dimeglumine (Magnevist, Bayer Healthcare). Dynamic injection of 0.1 mmol Magnevist per kilogram body weight was administered through power injector (Spectris, Medrad, Pittsburgh, PA) at a rate of 2 mL/s followed by a 20 mL saline flush also at a rate of 2 mL/s. A 1 mL test bolus was administered to determine the time to peak arterial enhancement of the aorta at the level of the celiac artery. Imaging was performed in arterial phase, portal venous, and equilibrium phases (at time to peak determine by test bolus, and at delay of 60 and 180 seconds, respectively).

Immediately after completion of equilibrium phase postcontrast acquisition, 3 additional VIBE acquisitions were performed: free-breathing radial VIBE, free-breathing conventional VIBE with 4 signal averages, and conventional BH VIBE. The 3 acquisitions were performed in random order with matching sequence parameters as follows: slice thickness 3 mm, flip angle 12 degrees, TR/TE 3.56–3.62 milliseconds/1.51–1.55 milliseconds, 80 axial slices, BW 590–610 Hz/pix, voxel size 1.6 × 1.6 × 3 mm, quick fat-saturation mode. A parallel-imaging factor of 2 was used for conventional VIBE only. For radial VIBE, 400 radial views were acquired in 4 interleaves (100 views/interleave) using the stack-of-stars scheme, where partitions were sampled sequentially for each view angle (Fig. 1). Parallel imaging was not used for radial VIBE acquisition. Image reconstruction for the radial VIBE data was done online at the scanner with a standard gridding procedure that included a correction of k-space shifts caused by gradient timing imperfections. Acquisition time for BH VIBE was 14 seconds. For the 2 acquisitions performed during free breathing, radial VIBE and VIBE with 4 averages, the acquisition time was 56 seconds each.

Image Data Analysis

All image data sets were stripped of the patient and acquisition parameter details and presented in a blinded fashion and in random order to 3 board-certified radiologists with 3, 5, and 8 years of abdominal MRI experience, respectively, who evaluated all images independently using a commercially available workstation (Syngo MultiModality Workplace, Siemens Healthcare, Erlangen, Germany).

For each data set, each reader independently scored following parameters of image quality using a scale of 1 to 5, with the highest score indicating the most desirable examination: overall image quality, respiratory motion artifact, pulsation artifact, liver edge sharpness, and hepatic vessel clarity (Table 1). Streak artifact was also scored using a 3-point scale, where 3 represented no artifact (Table 1).

To assess for image quality in the z-axis plane, axial data sets were reconstructed in the coronal plane as 4-mm thick section. Two readers blinded to the acquisition scheme evaluated overall image quality using a 5-point scale in consensus.

Statistical Analysis

Mixed model analysis of variance was used to compare sequences in terms of each measure of image quality. In each case, the ratings provided by the 3 readers for the 3 sequences served as the dependent variable and the model included reader as a blocking

TABLE 1. Scoring System of Image Quality Parameters

Image Quality Parameter	Score	Scoring System
Overall image quality	1–5	1. Unacceptable; 2. Poor; 3. Acceptable; 4. Good; 5. Excellent
Respiratory motion artifact	1–5	1. Unreadable; 2. Extreme artifact; 3. Moderate artifact; 4. Mild artifact; 5. None
Pulsation artifact	1–5	1. Unreadable; 2. Extreme artifact; 3. Moderate artifact; 4. Mild artifact; 5. None
Liver Edge sharpness & Hepatic vessel clarity	1–5	1. Unreadable; 2. Extreme blur; 3. Moderate blur; 4. Mild blur; 5. No blur
Streak artifact	1–3	1. Degrades image quality; 2. Artifact present but does not significantly degrade image quality; 3. No artifact

factor and sequence as a fixed classification factor. The inclusion of reader allowed sequence comparisons to be made within reader and then averaged over readers thereby accounting for any systematic differences between readers in terms of their propensities to assign lower or higher scores when assessing the same patient. To account for statistical dependencies among the ratings derived for the same patient, subject ID was incorporated into the analysis as a random classification factor. As a result, the correlation structure was modeled by assuming observations to be correlated only when acquired from the same subject. All reported P values were 2-sided and statistical significance was defined as $P < 0.05$. SAS 9.0 (SAS Institute, Cary, NC) was used for all computations.

RESULTS

All patients tolerated the MR examination and performed adequate breath-holds. One of the 18 patients did not undergo free-breathing acquisitions with multiple averages, and hence total of 53 acquisitions were reviewed by each reader.

Qualitative Evaluation

When comparing free-breathing radial VIBE against BH VIBE (Figs. 2, 3), we found that although there were differences between readers regarding absolute scores for each category (Table 2), the averaged scores across all readers showed no statistically significant differences (Table 3) in overall image quality ($P = 0.1015$), respiratory motion artifact ($P = 1.00$), and hepatic edge sharpness ($P = 0.2955$). Radial VIBE had significantly lower pulsation artifact compared with BH VIBE ($P < 0.0001$) but demonstrated lower score for hepatic vessel clarity ($P = 0.0176$) compared with BH VIBE. Streak artifact was seen only with radial VIBE (Fig. 4) and not with BH VIBE (1.6 ± 0.3 vs. 3.0; $P < 0.0001$).

Radial VIBE had significantly higher image quality parameter scores when compared with the alternative free-breathing approach, VIBE with multiple averages (Tables 2, 3) for overall image quality, respiratory motion artifact (Fig. 5), pulsation artifact, hepatic edge sharpness, and hepatic vessel clarity (all $P < 0.0001$). On most measures, the radial VIBE method averaged approximately 2 points better than VIBE with multiple averages (Table 3).

There was no statistically significant difference between coronal free-breathing radial VIBE and conventional BH VIBE regarding overall image quality (4.4 ± 0.6 vs. 4.5 ± 0.6; $P = 0.59$) (Fig. 6). Coronal free-breathing radial VIBE had significantly better image quality compared with free-breathing coronal conventional VIBE with multiple averages (4.4 ± 0.6 vs. 2.6 ± 0.9; $P < 0.0001$). No artifact was observed specifically only in the z-direction.

DISCUSSION

Our results demonstrate that clinical T1-weighted 3D examination of the liver is feasible with radial k-space sampling during free-breathing, and that overall image quality is similar to that of conventional BH VIBE acquisitions and significantly better compared with conventional free-breathing VIBE with multiple averages in patients undergoing postcontrast liver MRI.

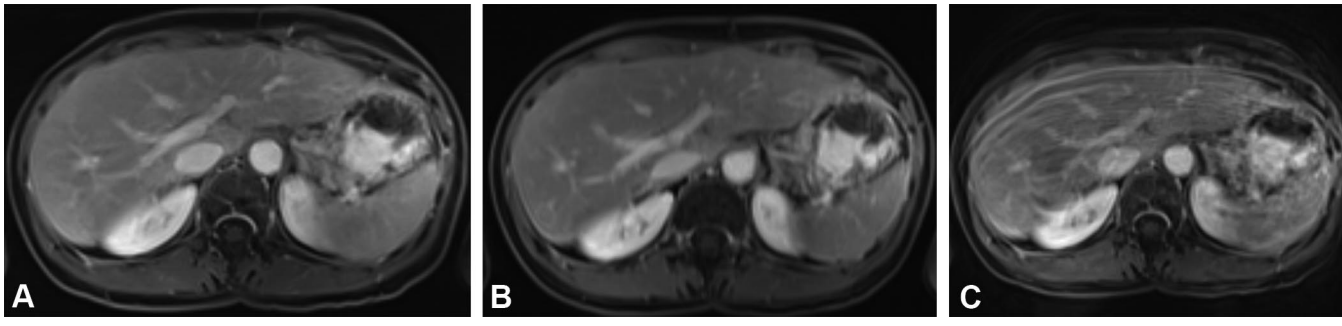

FIGURE 2. A 53-year-old man with prior history of orthotropic liver transplantation underwent examination of the liver after contrast administration with (A) free-breathing radial VIBE, (B) BH conventional VIBE, and (C) free-breathing conventional VIBE with multiple averages. Radial VIBE image quality was similar to that of BH conventional VIBE and significantly better than free-breathing conventional VIBE.

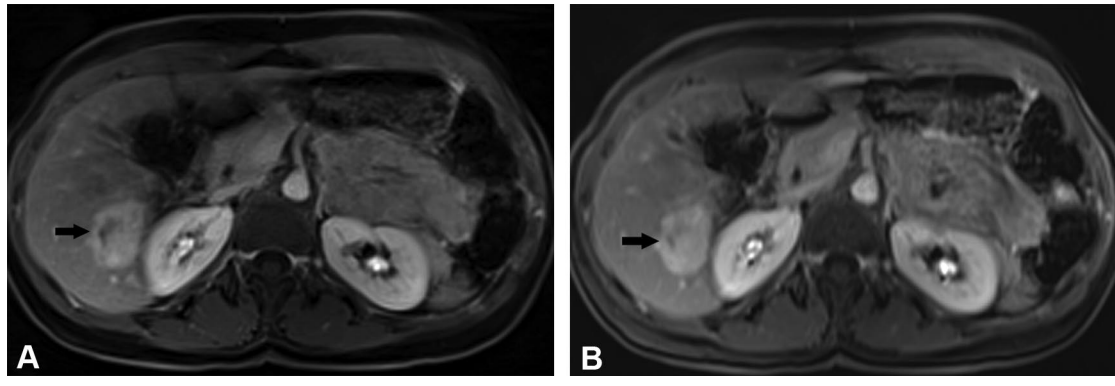

FIGURE 3. A 52-year-old woman presented for evaluation of a focal liver lesion. A, Free-breathing radial VIBE, and (B) conventional BH VIBE, demonstrate an enhancing lesion in the right lobe of the liver which was characterized as a hemangioma on dynamic postcontrast examination.

TABLE 2. Image Quality Parameter Scores for Each Reader and Each Sequence (Mean ± SD)*

	Reader 1			Reader 2			Reader 3		
Sequence	**BH**	**Radial**	**FB**	**BH**	**Radial**	**FB**	**BH**	**Radial**	**FB**
Overall image quality	4.5 ± 0.6	4.4 ± 0.6	2.3 ± 0.5	4.1 ± 1.0	3.7 ± 0.7	1.6 ± 0.7	3.5 ± 0.6	3.4 ± 0.6	1.7 ± 0.6
Respiratory motion artifact	4.8 ± 0.6	4.9 ± 0.2	2.5 ± 0.8	4.5 ± 0.8	4.2 ± 0.6	1.7 ± 0.8	4.7 ± 0.6	4.9 ± 0.3	2.1 ± 0.8
Pulsation artifact	4.1 ± 0.6	4.9 ± 0.2	2.3 ± 0.6	3.7 ± 1.0	5.0 ± 0	2.1 ± 0.9	3.7 ± 0.7	4.7 ± 0.7	2.6 ± 0.9
Hepatic edge sharpness	4.9 ± 0.2	4.7 ± 0.6	2.8 ± 0.9	4.4 ± 0.9	4.1 ± 0.5	2.5 ± 1.0	3.8 ± 0.6	4.0 ± 0.5	2.5 ± 0.8
Hepatic vessel clarity	4.6 ± 0.6	4.4 ± 0.6	2.1 ± 1.1	3.8 ± 0.9	3.6 ± 0.5	1.9 ± 0.9	3.6 ± 0.7	3.3 ± 0.6	2.2 ± 0.8

*Image quality parameter scores, where 1 = unacceptable and 5 = excellent.
BH indicates Breath-hold conventional VIBE; FB, free-breathing conventional VIBE; Radial, free-breathing radially sampled VIBE.

TABLE 3. Image Quality Parameter Scores Averaged Over All 3 Readers (Mean ± SD)*

	Average Scores			*P*	
Sequence	**BH**	**Radial**	**FB**	**Radial vs. BH**	**Radial vs. FB**
Overall image quality	4.0 ± 0.7	3.9 ± 0.5	1.8 ± 0.5	0.1015	<0.0001
Respiratory motion artifact	4.7 ± 0.6	4.7 ± 0.3	2.1 ± 0.6	1.00	<0.0001
Pulsation artifact	3.8 ± 0.6	4.9 ± 0.2	2.3 ± 0.4	<0.0001	<0.0001
Hepatic edge sharpness	4.4 ± 0.5	4.3 ± 0.4	2.6 ± 0.7	0.2955	<0.0001
Hepatic vessel clarity	4.0 ± 0.6	3.7 ± 0.5	2.1 ± 0.9	0.0176	<0.0001

*Image quality parameter scores, where 1 = unacceptable and 5 = excellent.
BH indicates breath-hold conventional VIBE; FB, free-breathing conventional VIBE; Radial, free-breathing radially sampled VIBE.

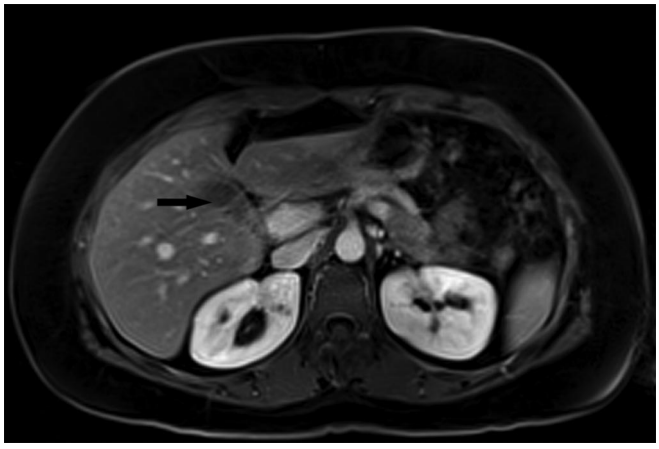

FIGURE 4. Free-breathing radial VIBE acquisition in a 30-year-old woman demonstrates streak artifacts (arrow) which slightly degrade image quality. These streak artifacts are not seen with conventional free-breathing VIBE, which was otherwise significantly inferior in image quality.

Significantly lower sensitivity to motion with the radial acquisition scheme is one of its distinct advantages. With conventional rectilinear k-space sampling, the spins differ by a constant phase offset for each sampled k-space line, classically known as the "phase-encoding" principle. Because translations in image space induce phase modulations of the k-space signal, motion effects disturb the constant phase offsets among sampled lines, which can be interpreted as displacing individual lines along the phase-encoding direction. Therefore, the Nyquist theorem is violated, leading to the appearance of dominant aliasing effects or ghosting. This problem is eliminated when sampling k-space along radial spokes, each with different readout directions. Therefore, motion artifacts present in the images as radially oriented streaks or mild blurring. Furthermore, the overlap of the radial spokes in the center of k-space has a time averaging effect that additionally reduces the sensitivity to motion and flow. As we observed, radial VIBE acquisitions result in significantly lower pulsation artifacts compared with BH and FB VIBE. These results are consistent with published studies which have demonstrated that radial schemes such as PROPELLER can improve image quality for 2D T2-weighted turbo spin-echo and diffusion-weighted imaging of the liver.[20–23,30] To our knowledge, this is the first report of feasibility and clinical application of such radial 3D fat-suppressed T1-weighted postcontrast acquisition in the abdomen. Our work demonstrates that the image quality of such radial free-breathing acquisition is similar to BH conventional rectilinear acquisition scheme.

One of the disadvantages of radial k-space sampling is streak artifact that results from undersampling and respiratory motion, which is not seen with conventional rectilinear VIBE acquisitions. Although the presence of streak artifacts degraded image quality in a number of cases, the images remained of diagnostic quality in all cases. Future work will focus on improving image reconstruction algorithms to further decrease streak artifacts and improve image quality.

In this study, all patients were deemed to be adequate breath-holders and hence in almost all cases the images acquired with BH acquisition scheme were of good diagnostic quality. However, in sick, elderly, and pediatric patient populations, subjects may have difficulty breath-holding for more than 10 seconds, resulting in contrast-enhanced images which are often nondiagnostic. In this patient population, free-breathing radial VIBE may serve as an excellent alternative to BH VIBE in providing diagnostic quality postcontrast imaging of the liver and upper abdomen.

Because of the robustness of the sequence to the motion, radial k-space sampling should be well suited for moving table acquisitions. Combination of moving table with a radial 3D sequence may not only make the acquisition robust to nonuniform table movement but also to patient motion during the scan. It may also be possible to integrate this radial sequence in MR-PET system. A key advantage of the MR-PET scanner is that it allows for a simultaneous acquisition of the PET and MRI data, which may help overcome registration problems that arise with fusing separately acquired MRI and PET data. A free-breathing motion robust scanning approach similar to the radial VIBE sequence may improve the quality of the MRI and PET fusion due to absence of ghosting artifacts and because similar to PET acquisition it is acquired during

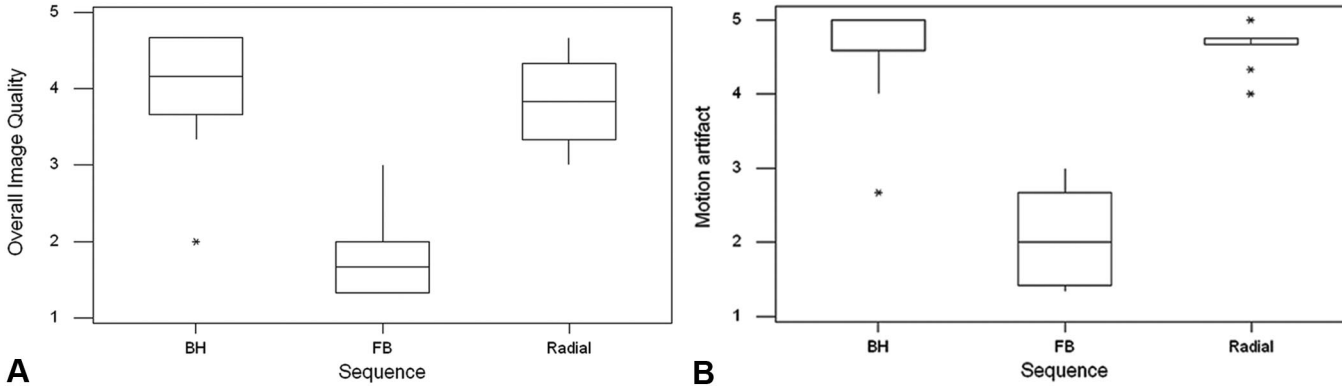

FIGURE 5. Box-plot of (A) overall image quality, and (B) respiratory motion artifact scores averaged over 3 readers for conventional BH VIBE, free-breathing VIBE with multiple averages (FB), and free-breathing radial VIBE (radial). Top and bottom of boxes represent 25 to 75 percentiles of the data values. Line in box represents median value.

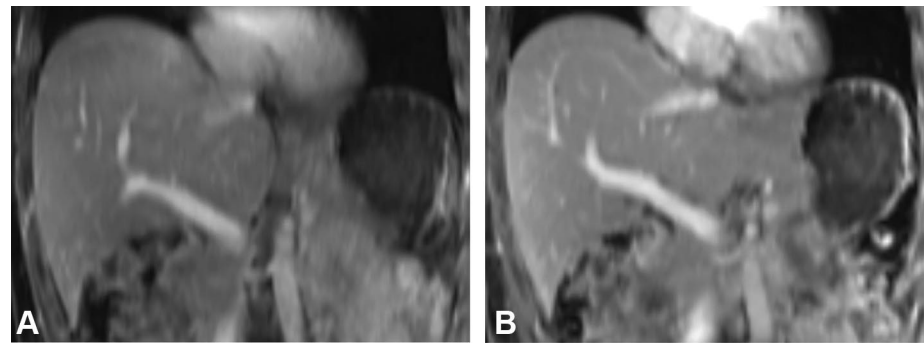

FIGURE 6. Coronal reformatted (A) free-breathing radial VIBE and (B) conventional BH VIBE demonstrate similar image quality in a 32-year-old woman who underwent MRI examination for evaluation of a suspected liver lesion.

free-breathing. These potential applications of radial VIBE are exciting and require systematic evaluation. Furthermore, high-resolution free-breathing radial acquisition after administration of hepatobiliary contrast agent may have important application in detection of small liver metastasis in patient with primary malignancy, and this also needs to be prospectively assessed.

Currently, one of the limitations of the radial VIBE acquisition is the relatively long acquisition time of close to one minute that limits its utility for dynamic liver imaging, which requires multiphase acquisition (in arterial, portal venous, and equilibrium phase) with temporal resolution of about 10 to 20 seconds. We performed radial VIBE imaging with a high number of radial views (100 views per interleave with total of 400 views). However, with improvements in reconstruction algorithms it may be possible to further decrease the number of views needed for diagnostic quality images, which will result in shortened acquisition times. One such approach is the use of compressed sensing reconstruction algorithms, with promising early results.[31–33] Implementation of parallel imaging may also help to lower the acquisition time.

Another possibility is the use of a recently described view-sharing technique for radial sampling, k-space-weighted image contrast (KWIC), which permits manipulation of image contrast by judicious temporal filtering of the acquired views. This allows for reconstructions with arbitrary temporal resolutions from a single dynamic contrast-enhanced examination during postprocessing.[29] In the present study, radial VIBE data were acquired using 4 interleaves with 100 radial views per interleave where all 400 views were used in generating a single full-dataset (high signal-to-noise) image. However, it is possible to retrospectively reconstruct subframe images with temporal resolution of 14 seconds by using only the 100 views from each individual interleave and complementing the undersampled data with peripheral k-space information from the other interleaves. The KWIC approach was initially proposed for dynamic imaging of the breast,[34] and, if validated for liver imaging, it could potentially eliminate the need for multiple BH acquisitions during postcontrast dynamic imaging. This would result in improved patient comfort and efficient scanning. However, KWIC reconstruction needs further optimization as decreasing number of views (undersampling) leads to streak artifacts and there is some temporal bleeding due to view sharing employed with KWIC reconstruction. When some of these issues are resolved, the next step certainly will be to perform dynamic imaging of the liver.

Our study has other limitations. We imaged a small number of subjects (n = 18), and imaging was performed in the delayed phase of acquisition only. Therefore, clinical utility for evaluating lesions remains to be validated. However, the purpose of our study was to compare image quality of free-breathing radial VIBE to conventional BH and free-breathing VIBE acquisitions. A prospective study in a larger patient population is planned to assess the diagnostic utility for focal lesion detection and characterization. We compared radial VIBE against a VIBE acquisition with multiple averages. Some have also advocated a 2D fast low-angle shot (FLASH) gradient echo or turbo FLASH sequence for non-BH liver imaging. We chose not to incorporate this sequence in our study because of its substantially lower spatial resolution, inability to perform good quality multiplanar reformation, and the inability to perform high-quality fat suppression with this sequence.

In conclusion, we have demonstrated the potential utility of a 3D radial VIBE technique for postcontrast liver MRI performed during free breathing which is comparable in image quality to BH

VIBE and significantly better than conventional VIBE performed with multiple averages during free breathing. In patient populations that have difficulty with BHs longer than 10 seconds, this technique may be a valuable imaging strategy. A prospective study is planned to assess the diagnostic utility of free-breathing radial VIBE acquisition for focal lesion detection and characterization.

REFERENCES

1. Schultz CL, Alfidi RJ, Nelson AD, et al. The effect of motion on two-dimensional Fourier transformation magnetic resonance images. *Radiology*. 1984;152:117–121.
2. Axel L, Summers RM, Kressel HY, et al. Respiratory effects in two-dimensional Fourier transform MR imaging. *Radiology*. 1986;160:795–801.
3. Ehman RL, McNamara MT, Brasch RC, et al. Influence of physiologic motion on the appearance of tissue in MR images. *Radiology*. 1986;159:777–782.
4. Wood ML, Henkelman RM. Suppression of respiratory motion artifacts in magnetic resonance imaging. *Med Phys*. 1986;13:794–805.
5. Wood ML, Henkelman RM. MR image artifacts from periodic motion. *Med Phys*. 1985;12:143–151.
6. Low RN, Alzate GD, Shimakawa A. Motion suppression in MR imaging of the liver: comparison of respiratory-triggered and nontriggered fast spin-echo sequences. *Am J Roentgenol*. 1997;168:225–231.
7. Paling MR, Brookeman JR. Respiration artifacts in MR imaging: reduction by breath holding. *J Comput Assist Tomogr*. 1986;10:1080–1082.
8. Maki JH, Chenevert TL, Prince MR. The effects of incomplete breath-holding on 3D MR image quality. *J Magn Reson Imaging*. 1997;7:1132–1139.
9. Keogan MT, Edelman RR. Technologic advances in abdominal MR imaging. *Radiology*. 2001;220:310–320.
10. Ehman RL, McNamara MT, Pallack M, et al. Magnetic resonance imaging with respiratory gating: techniques and advantages. *Am J Roentgenol*. 1984; 143:1175–1182.
11. Runge VM, Clanton JA, Partain CL, et al. Respiratory gating in magnetic resonance imaging at 0.5 Tesla. *Radiology*. 1984;151:521–523.
12. Ehman RL, Felmlee JP. Adaptive technique for high-definition MR imaging of moving structures. *Radiology*. 1989;173:255–263.
13. Groch MW, Turner DA, Erwin WD. Respiratory gating in magnetic resonance imaging: improved image quality over non-gated images for equal scan time. *Clin Imaging*. 1991;15:196–201.
14. Sinkus R, Bornert P. Motion pattern adapted real-time respiratory gating. *Magn Reson Med*. 1999;41:148–155.
15. Klessen C, Asbach P, Kroencke TJ, et al. Magnetic resonance imaging of the upper abdomen using a free-breathing T2-weighted turbo spin echo sequence with navigator triggered prospective acquisition correction. *J Magn Reson Imaging*. 2005;21:576–582.
16. Brau AC, Brittain JH. Generalized self-navigated motion detection technique: preliminary investigation in abdominal imaging. *Magn Reson Med*. 2006;55: 263–270.
17. Taouli B, Sandberg A, Stemmer A, et al. Diffusion-weighted imaging of the liver: comparison of navigator triggered and breathhold acquisitions. *J Magn Reson Imaging*. 2009;30:561–568.
18. Mitchell DG, Vinitski S, Burk DL Jr, et al. Motion artifact reduction in MR imaging of the abdomen: gradient moment nulling versus respiratory-sorted phase encoding. *Radiology*. 1988;169:155–160.
19. Haacke EM, Lenz GW. Improving MR image quality in the presence of motion by using rephasing gradients. *Am J Roentgenol*. 1987;148:1251–1258.
20. Hirokawa Y, Isoda H, Maetani YS, et al. Evaluation of motion correction effect and image quality with the periodically rotated overlapping parallel lines with enhanced reconstruction (PROPELLER) (BLADE) and parallel imaging acquisition technique in the upper abdomen. *J Magn Reson Imaging*. 2008;28:957–962.
21. Deng J, Miller FH, Salem R, et al. Multishot diffusion-weighted PROPELLER magnetic resonance imaging of the abdomen. *Invest Radiol*. 2006;41:769–775.
22. Deng J, Omary RA, Larson AC. Multishot diffusion-weighted SPLICE PROPELLER MRI of the abdomen. *Magn Reson Med*. 2008;59:947–953.
23. Hirokawa Y, Isoda H, Maetani YS, et al. MRI artifact reduction and quality improvement in the upper abdomen with PROPELLER and prospective acquisition correction (PACE) technique. *Am J Roentgenol*. 2008;191:1154–1158.
24. Elsayes KM, Narra VR, Yin Y, et al. Focal hepatic lesions: diagnostic value of enhancement pattern approach with contrast-enhanced 3D gradient-echo MR imaging. *Radiographics*. 2005;25:1299–1320.
25. Quillin SP, Atilla S, Brown JJ, et al. Characterization of focal hepatic masses by dynamic contrast-enhanced MR imaging: findings in 311 lesions. *Magn Reson Imaging*. 1997;15:275–285.
26. Young PM, Brau AC, Iwadate Y, et al. Respiratory navigated free breathing 3D spoiled gradient-recalled echo sequence for contrast-enhanced examination of the liver: diagnostic utility and comparison with free breathing and breath-hold conventional examinations. *Am J Roentgenol*. 2010;195:687–691.
27. Vasanawala SS, Iwadate Y, Church DG, et al. Navigated abdominal T1-W MRI permits free-breathing image acquisition with less motion artifact. *Pediatr Radiol*. 2010;40:340–344.
28. Lin W, Guo J, Rosen MA, et al. Respiratory motion-compensated radial dynamic contrast-enhanced (DCE)-MRI of chest and abdominal lesions. *Magn Reson Med*. 2008;60:1135–1146.
29. Song HK, Dougherty L. Dynamic MRI with projection reconstruction and KWIC processing for simultaneous high spatial and temporal resolution. *Magn Reson Med*. 2004;52:815–824.
30. Hirokawa Y, Isoda H, Okada T, et al. Improved detection of hepatic metastases from pancreatic cancer using periodically rotated overlapping parallel lines with enhanced reconstruction (PROPELLER) technique after SPIO administration. *Invest Radiol*. 2010;45:158–164.
31. Lustig M, Donoho D, Pauly JM. Sparse MRI: The application of compressed sensing for rapid MR imaging. *Magn Reson Med*. 2007;58:1182–1195.
32. Block KT, Uecker M, Frahm J. Undersampled radial MRI with multiple coils. Iterative image reconstruction using a total variation constraint. *Magn Reson Med*. 2007;57:1086–1098.
33. Otazo R, Kim D, Axel L, et al. Combination of compressed sensing and parallel imaging for highly accelerated first-pass cardiac perfusion MRI. *Magn Reson Med.* 64:767–776.
34. Dougherty L, Isaac G, Rosen MA, et al. High frame-rate simultaneous bilateral breast DCE-MRI. *Magn Reson Med*. 2007;57:220–225.